

1
2
3
4
5
6
7
8
9
10
11
12
13
14
15
16
17
18
19
20
21
22
23
24
25
26
27
28
29
30
31
32
33
34
35
36
37
38
39
40
41
42
43
44
45
46
47
48
49
50
51
52
53
54
55
56
57
58
59
60

Acyl Carrier Protein Cyanylation Delivers a Ketoacyl Synthase-Carrier Protein Crosslink

Grace A. Thiele,^[a] Connie P. Friedman,^[a] Kathleen J. S. Tsai,^[a] Joris Beld,^[b] Casey H. Londergan,^{[a]*} Louise K. Charkoudian^{[a]*}

^[a]Department of Chemistry, Haverford College, Haverford Pennsylvania 19041-1392 USA

^[b]Department of Microbiology and Immunology, Drexel University College of Medicine, 245 N 15th St, Philadelphia, PA 19102.

Acyl carrier protein, ketoacyl synthase, polyketide biosynthesis, fatty acid synthase, mechanism-based crosslink, vibrational spectroscopic probes, thiocyanate

Supporting Information Placeholder

ABSTRACT: Acyl carrier proteins (ACPs) are central hubs in polyketide and fatty acid biosynthetic pathways, but the fast motions of the ACP's phosphopantetheine (Ppant) arm make its conformational dynamics difficult to capture using traditional spectroscopic approaches. Here we report that converting the terminal thiol of *E. coli* ACP's Ppant arm into a thiocyanate activates this site to form a selective crosslink with the active site cysteine of its partner ketoacyl synthase (KS; FabF). The reaction releases a cyanide anion, which can be detected by infrared spectroscopy. This represents a practical and generalizable method to obtain and visualize ACP-protein complexes relevant to biocatalysis and will be valuable in future structural and engineering studies.

Polyketide synthases (PKSs) and fatty acid synthases (FASs) produce structurally diverse molecules with pharmacologically relevant properties. Acyl carrier proteins (ACPs) play a central role in these synthases by using their 18 Å-long 4'-phosphopantetheine (Ppant) arm to shuttle building blocks and intermediates to appropriate catalytic partners to carry out the chemistries programmed by the synthase (Figure 1A). The fast motions of ACPs enable the protein to protect and present its molecular cargo as needed, but also make it difficult to study its structure and its interactions with

other proteins.¹ Here we report a practical method to obtain and visualize ACP-protein interactions relevant to catalysis. We anticipate that this method will be valuable in future structural and engineering studies.

We recently reported that converting the ACP Ppant arm's thiol to a thiocyanate (ACP-SCN) turns the reactive end of the arm into a probe that reports on hydrogen bonding and local dynamics (Figure 1B).² The frequency of the thiocyanate band is sensitive to the local solvation environment: when the Ppant arm of ACP-SCN is solvent exposed it absorbs at ~2163 cm⁻¹, but when the arm is buried the probe band exhibits a red-shift of 5-10 cm⁻¹. Since the Ppant arm can enter the hydrophobic active site of catalytic partners,^{1,3} we hoped that this catalytically relevant change of solvation environment could be traced with the solvato-sensitive thiocyanate probe (Figure 1C).

To test this hypothesis, we identified a model ACP/partner system: the *E. coli* fatty acid ACP, AcpP, and one of its cognate KSs, FabF. During the fatty acid elongation cycle in *E. coli*, AcpP collaborates with FabF to catalyze a Claisen condensation reaction that extends the growing alkyl chain by two carbon units. While characterizing the AcpP-FabF interaction is paramount to understanding and manipulating FASs, the AcpP-FabF

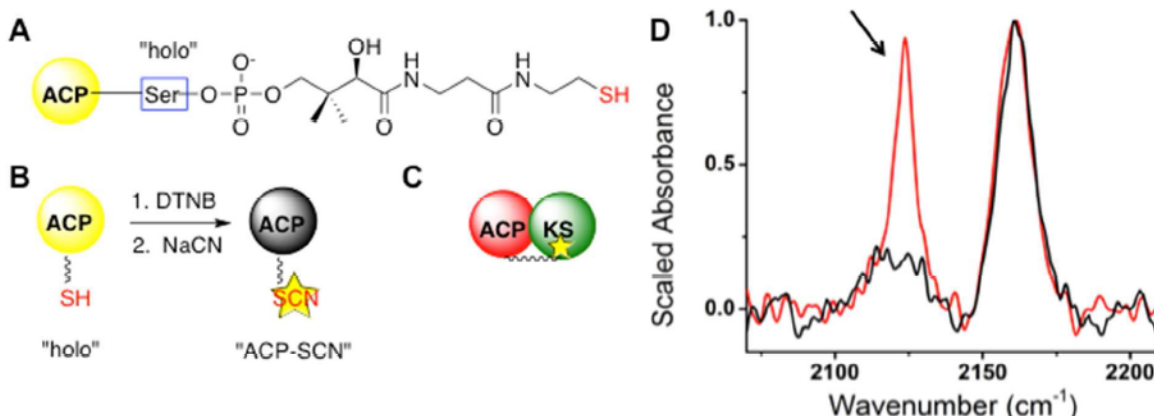


Figure 1. The thiol of the ACP P pant arm (A) is converted into thiocyanate via a one-pot cyanylation reaction (B). We hypothesized that the labeled P pant arm would gain access to the active site of cognate ketoacyl synthase (KS) enzymes (C), and that this change in solvation could be monitored by vibrational spectroscopy. IR analysis of cyanylated *E. coli* ACP, AcpP-SCN, titrated with its cognate KS (FabF) supports this hypothesis (D). The infrared CN stretching band of AcpP-SCN (black) absorbs at 2161 cm^{-1} , a frequency consistent with the label being water exposed.² When AcpP-SCN was titrated with FabF a new peak at 2120 cm^{-1} (arrow) was observed.

interaction is difficult to study due to its transient nature. To overcome this obstacle, Burkart and coworkers used solvatochromatic fluorescence and crosslinking studies to visualize the movement of the AcP P pant arm into the hydrophobic active site of FabF.^{4,5} That work confirmed that the AcP P pant arm experiences a change in solvation environment (from solvent exposed to solvent excluded) upon its interaction with FabF, and validate the use of the AcP/FabF pair to test our hypothesis.

We labeled AcP with the thiocyanate probe to make the product AcpP-SCN and found that cyanylation did not perturb the protein's helical structure (Figure S1). AcpP-SCN exhibited a mode frequency of 2161 cm^{-1} , which based on prior results from model molecules⁶ and proteins² suggests that the P pant arm is mainly solvent exposed in the absence of a catalytic partner (Figure 1D).

We predicted that the interaction between AcpP-SCN and FabF would induce a red shift of 6-7 cm^{-1} in the CN frequency of AcpP-SCN when the probe entered the solvent-excluded FabF active site. To our surprise, the introduction of FabF resulted in a decrease in intensity of the 2161 cm^{-1} band and an appearance of a new peak at 2120 cm^{-1} (Figure 1D). The 40 cm^{-1} shift in the CN stretching band indicated that the interaction of AcpP-SCN with FabF chemically transformed the CN-containing functional group.

We hypothesized that the band at 2120 cm^{-1} was

due to free CN^- released from the SCN group. To test this theory, we repeated the titration experiment using AcpP-S¹³CN, where the isotopic mass of carbon-13 would lead to a lower vibrational frequency of any bonds containing the carbon atom of the thiocyanate. Both the AcpP-S¹³CN alone and AcpP-S¹³CN treated with FabF displayed ¹³C isotope frequency shifts of -50 cm^{-1} vs natural abundance (Figure S2), indicating that the new band at 2120 cm^{-1} in Figure 1D is due to a mode containing the thiocyanate carbon atom.⁷ Further support for assignment of the 2120 cm^{-1} band to CN^- released from the SCN group includes the observation of this peak upon titration of FabF with NaCN in the absence of AcP (data not shown).

We postulated that CN^- was released upon the formation of a crosslinked FabF-AcpP complex, and therefore analyzed the reaction mixture using size exclusion chromatography (SEC; Figure 2A). For AcpP-SCN, we observed two peaks in the chromatogram (18 and 22 min), corresponding to the known equilibrium of the monomer and dimer AcP states under non-reducing conditions.⁸ Titration of AcpP-SCN with FabF resulted in a decrease in these peaks and the appearance of a complex larger than FabF alone eluting at 16 minutes, consistent with the formation of a FabF-AcpP adduct.

The most likely covalent link between AcP and FabF is via a disulfide bond resulting from the FabF active site (Cys163) attacking AcpP-SCN's sulfur atom, releasing free CN^- , as shown in Figure 2A. To test this model, we titrated AcpP-SCN with

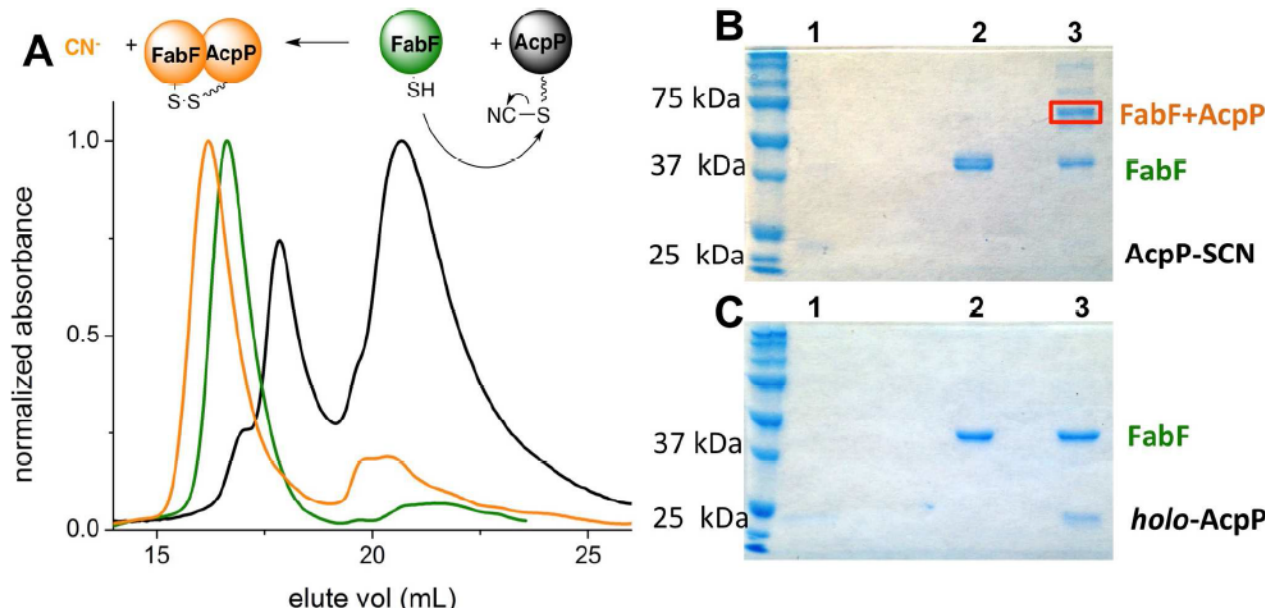


Figure 2. Size-exclusion chromatography (280 nm) shows that when AcP-SCN (black) is titrated with FabF (green) a higher molecular weight complex is formed (orange) (A). AcP partly forms a dimeric complex under non-reducing conditions,⁸ giving rise to two peaks in the chromatogram. The complex eluting at 16 mL was collected and analyzed via non-reducing (B) and reducing (C) SDS PAGE gels (lane 1 = AcP; lane 2 = FabF; lane 3 = complex at 16 mL). The disappearance of the high molecular weight complex (red box) and the increase in intensity of AcP/FabF bands observed under reducing conditions, support that AcP and FabF are linked via a disulfide bond.

FabF and analyzed the product via gel electrophoresis in the presence and absence of a disulfide reducing agent. We observed the covalent cross-linked product via gel electrophoresis under non-reducing conditions, but not reducing conditions (Figures 2B,C and S3).

To determine if the disulfide crosslink occurred at Cys163, we titrated AcP-SCN with FabF pre-incubated with cerulenin, an inhibitor of the FabF KS active site cysteine.⁹ SDS PAGE analysis showed that the inhibited FabF does not form a crosslink with AcP-SCN (Figure S4). The 2120 cm^{-1} IR band was not observed, indicating that the CN⁻ release requires that AcP's Ppant arm enter the FabF active site (Figure S4). The attachment point between AcP and FabF was further confirmed by tandem proteolysis mass spectrometry: digestion of the crosslinked product with trypsin and chymotrypsin yields a product consistent with a FabF peptide fragment tethered to an AcP peptide fragment via a disulfide bond between the FabF Cys163 active site and AcP Ppant arm (Figures S5-S10).

Reactions of cysteine sulfenyl thiocyanates with thiols are known to afford unsymmetrical disulfides.¹⁰ While the resultant disulfides are typically only stable in protic solvents under very acidic conditions, it appears that this reaction can take place within the active site of FabF, and that the local environment facilitates the formation of the FabF-

AcpP disulfide bond. Since unlabeled *holo*-AcpP does not readily form a crosslink with FabF *in vitro* (Figure S11), we speculate that the cyanylation of AcP either mimics a nascent substrate and induces a conformational change that alters the orientation of AcP with respect to KS,¹¹ or facilitates crosslinking via an S_N2-type reaction by providing a robust leaving group. Once the arm is “activated”, a stable Ppant-Cys crosslink can be formed, as observed previously *in vivo*,¹² and in engineered non-ribosomal peptide synthetase systems.¹³

The simple installation of a thiocyanate probe on the AcP Ppant arm provides a reactive and spectroscopically unique handle that facilitates the creation of a mechanistically relevant FabF-AcpP cross-linked product. IR spectroscopy using relatively conventional commercial instrumentation can be used to monitor formation of the crosslinked product via release of CN⁻. To extend the potential impact of these findings, we investigated whether other ACPs could be crosslinked to FabF via this cyanylation approach, and if the appearance of an IR peak at 2120 cm^{-1} could serve as a general readout for productive FabF-ACP interactions. Previous studies showed that FabF productively interacts with the polyketide ACP from frenolicin biosynthesis (ACP_{fren}), but not the polyketide ACP from actinorhodin biosynthesis (ACP_{act}).¹⁴ Thus, if FabF-ACP crosslinks were selectively formed when FabF is titrated with a functional cyanlated ACP,

1 we would expect to see evidence of a covalent
2 crosslink and release of CN⁻ for ACP_{fren} but not
3 ACP_{act}. Indeed, titration of ACP_{fren}-SCN with FabF
4 led to a crosslinked product (Figure S12) also
5 marked by CN⁻ in the IR spectrum (Figure S13).
6 Titration of ACP_{act}-SCN with FabF neither afforded
7 a crosslink (Figure S12) nor the release of CN⁻
8 (Figure S13). Similarly, no crosslink or 2120 cm⁻¹
9 peak was observed upon titration of ACP-SCN with
10 a bovine serum albumin (BSA) protein control (data
11 not shown). These data show that the crosslinking
12 reaction between ACP-SCN and FabF is selective
13 to functional interactions and could potentially be
14 used to monitor ACP interactions with other cognate
15 catalytic partners.

16 The thiocyanate-facilitated crosslinking of ACPs to
17 FabF is a practical method to obtain protein complexes
18 relevant to biocatalysis. Previous efforts to
19 visualize AcpP-protein interactions required isotopic
20 labeling, multi-step synthesis of pantetheine-
21 based probes, and/or chemoenzymatic loading of
22 synthetic probes onto AcpP.^{15,16} While these
23 approaches can target ACP interactions with diverse
24 catalytic partners, the thiocyanylation with IR method
25 offers an alternative in which the simple bio-
26 orthogonal modification of AcpP activates the protein
27 for covalent linkage to FabF, and possibly other
28 enzymes containing an active site cysteine.

29 Future work will focus on using this method to obtain
30 crystal structures of FabF-ACP complexes and
31 identify residues that guide functional interactions.
32 The ability to visualize functional FabF-ACP interactions
33 *in situ* via the presence/absence of a peak
34 in the IR at 2120 cm⁻¹ will also be explored as a
35 low-barrier tool to screen functional unnatural bio-
36 synthetic partners. Given that cyanylation of ACPs and
37 IR spectroscopy are amenable to high throughput
38 approaches, these methods could enable rapid
39 progress towards building hybrid synthases capable
40 of creating new chemical diversity.

41 ASSOCIATED CONTENT

42 Supporting information (methods and figures) is
43 available free of charge at <http://pubs.acs.org>.

44 AUTHOR INFORMATION

45 Corresponding Authors

46 *lcharkou@haverford.edu; clonderg@haverford.edu

47 Funding Sources

48 We gratefully acknowledge the Research Corporation
49 for Scientific Advancement Cottrell College Science
50 Award (L.K.C.), NIH R15GM120704 (L.K.C.), NSF
51

52 CAREER grant CHE-1652424 (L.K.C.), NSF
53 CAREER grant CHE-1150727 (CHL), a Henry Dreyfus
54 Teacher-Scholar Award (CHL), summer research
55 fellowships from Haverford College (K.J.S.T., G.A.T.,
56 C.P.F) and B.A. Rudolph Foundation (K.J.S.T.). The
57 content is solely the responsibility of the authors and
58 does not necessarily represent the views of the NIH
59 or
60 NSF.

Notes

No competing financial interests have been declared.

ACKNOWLEDGMENT

We thank Dr. Hsin-Yao Tang at the Wistar Institute Proteomics and Metabolomics Facility for analysis of proteomics data, and Prof. Chaitan Khosla for generously providing FabF and AcpP expression plasmids.

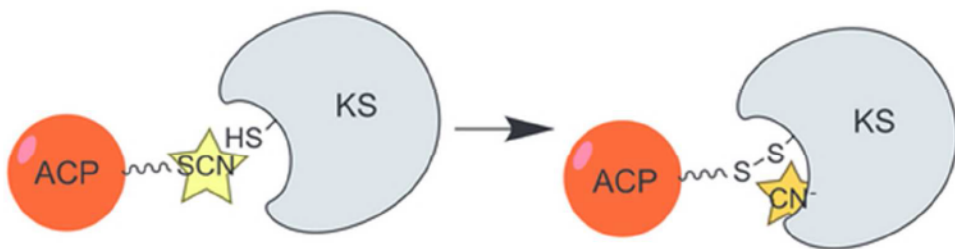
ABBREVIATIONS

ACP, acyl carrier protein; FAS, fatty acid synthase; IR, infrared; KS, ketoacyl synthase PKS, polyketide synthase; Ppant, phosphopantetheine; size exclusion chromatography (SEC).

REFERENCES

- (1) Cronan, J. E. (2014) *Biochem. J.* **460**, 157–163.
- (2) Johnson, M. N. R., Londergan, C. H., Charkoudian, L. K. (2014) *J. Am. Chem. Soc.* **136**, 11240–11243.
- (3) Nguyen, C., Haushalter, R. W., Lee, D. J., Markwick, P. R. L., Bruegger, J., Caldara-Festin, G., Finzel, K., Jackson, D. R., Ishikawa, F., O'Dowd, B., McCammon, J. A., Opella, S. J., Tsai, S.-C., Burkart, M. D. (2014) *Nature* **505**, 427–431.
- (4) Beld, J., Cang, H., Burkart, M. D. (2014) *Angew. Chem. Int. Ed.* **53**, 14456–14461.
- (5) Worthington, A. S., Porter, D. F., Burkart, M. D. (2010) *Org. Biomol. Chem.* **8**, 1769.
- (6) Maienschein-Cline, M. G., Londergan, C. H. (2007) *J. Phys. Chem. A* **111**, 10020–10025.
- (7) Yoshikawa, S., O'Keefe, D. H., Caughey, W. S. (1985) *J. Biol. Chem.* **260**, 3518–3528.
- (8) Keating, D. H., Cronan, J. E. (1996) *J. Biol. Chem.* **271**, 15905–15910.
- (9) Moche, M., Schneider, G., Edwards, P., Dehesh, K., Lindquist, Y. (1999) *J. Biol. Chem.* **274**, 6031–6034.
- (10) Alguindigue Nimmo, S. L., Lemma, K., Ashby, M. T. (2007) *Heteroatom Chem.* **18**, 467–471.
- (11) Whicher, J. R., Dutta, S., Hansen, D. A., Hale, W. A., Chemler, J. A., Dosey, A. M., Narayan, A. R. H., Håkansson, K., Sherman, D. H., Smith, J. L., Skiniotis, G. (2014) *Nature* **510**, 560–564.
- (12) Rock, C. O. (1982) *J. Bacteriol.* **152**, 1298–1300.
- (13) Tarry, M. J., Schmeing, T. M. (2015) *Protein Eng. Des. Sel.* **28**, 163–170.
- (14) Bruegger, J., Haushalter, B., Vagstad, A., Shakya, G., Mih, N., Townsend, C. A., Burkart, M. D., Tsai, S.-C. (2013) *Chem. Biol.* **20**, 1135–1146.
- (15) Finzel, K., Lee, D. J., Burkart, M. D. (2015) *ChemBioChem* **16**, 528–547.
- (16) Beld, J., Lee, D. J., Burkart, M. D. (2014) *Mol. BioSyst.* **11**, 38–59.

1
2
3
4
5
6
7
8
9
10
11
12
13
14
15
16
17
18
19
20
21
22
23
24
25
26
27
28
29
30
31
32
33
34
35
36
37
38
39
40
41
42
43
44
45
46
47
48
49
50
51
52
53
54
55
56
57
58
59
60



For Table of Contents use only

43x11mm (300 x 300 DPI)

